Biomaterials Science

REVIEW

View Article Online
View Journal | View Issue

Cite this: *Biomater. Sci.*, 2017, **5**, 632

Microvalve-based bioprinting – process, bio-inks and applications

Wei Long Ng,[a,b] Jia Min Lee,[a] Wai Yee Yeong*[a] and May Win Naing[b]

Bioprinting is an emerging research field that has attracted tremendous attention for various applications; it offers a highly automated, advanced manufacturing platform for the fabrication of complex bio-engineered constructs. Different bio-inks comprising multiple types of printable biomaterials and cells are utilized during the bioprinting process to improve the homology to native tissues and/or organs in a highly reproducible manner. This paper, presenting a first-time comprehensive yet succinct review of microvalve-based bioprinting, provides an in-depth analysis and comparison of different drop-on-demand bioprinting systems and highlights the important considerations for microvalve-based bioprinting systems. This review paper reports a detailed analysis of its printing process, bio-ink properties and cellular components on the printing outcomes. Lastly, this review highlights the significance of drop-on-demand bioprinting for various applications such as high-throughput screening, fundamental cell biology research, *in situ* bioprinting and fabrication of *in vitro* tissue constructs and also presents future directions to transform the microvalve-based bioprinting technology into imperative tools for tissue engineering and regenerative medicine.

Received 27th November 2016,
Accepted 22nd January 2017

DOI: 10.1039/c6bm00861e

rsc.li/biomaterials-science

Introduction

Recent advances in 3D bioprinting facilitate the simultaneous deposition of biomaterials and living cells to directly create biomimetic 3D cell-material constructs that are biomimetic in macro-architecture.[1] 3D bioprinting can be defined as "the use of computer-aided transfer processes for patterning and assembling biologically-relevant materials with a prescribed

[a]*Singapore Centre for 3D Printing (SC3DP), School of Mechanical and Aerospace Engineering, Nanyang Technological University (NTU), 50 Nanyang Avenue, Singapore 639798, Singapore. E-mail: wyyeong@ntu.edu.sg*
[b]*Singapore Institute of Manufacturing Technology (SIMTech), Agency for Science, Technology and Research, 73 Nanyang Drive, Singapore 637662*

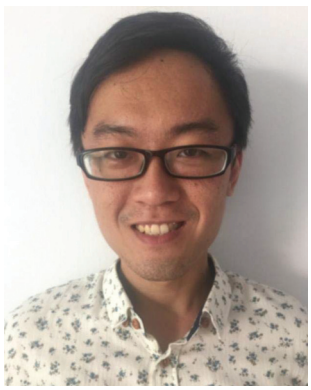

Wei Long Ng

*Wei Long Ng obtained his first degree in Bioengineering from Nanyang Technological University, Singapore. After receiving his BEng. (Hons) in 2013, he was awarded the A*STAR Graduate Scholarship to pursue his Ph.D. under the supervision of Dr May Win Naing and Assistant Professor Yeong Wai Yee in the School of Mechanical and Aerospace Engineering (MAE) at Nanyang Technological University. His research interest centers on developing novel bio-inks and engineering functional microenvironments for 3D-printed* in vitro *human tissue models.*

Jia Min Lee

Jia Min Lee received her BEng. (Hons) in Bioengineering from Nanyang Technological University in 2013. She is currently a research student under the supervision of Assistant Professor Yeong Wai Yee in the School of Mechanical and Aerospace Engineering (MAE) at Nanyang Technological University. Her research focuses on material formulation and design strategies for bioprinting of biological constructs.

organization to fabricate complex bioengineered structures".[2] it is a new fabrication paradigm that provides a highly automated manufacturing platform for the fabrication of complex bioengineered constructs *via* a layer-by-layer printing process with a high degree of flexibility and repeatability.[3] The biologically relevant material used in these bioprinting systems is known as "bio-ink". "Bio-ink" refers to a printable biomaterial consisting of various biologics (*i.e.* cells, growth factors or drugs) encapsulated within a delivery matrix such as culture media or hydrogels. Significant advances in 3D bioprinting research over the past decade have been recently highlighted by several excellent review papers.[4–7] These papers discussed the use of various AM processes and different printing strategies to fabricate 3D bioprinted constructs that closely resemble the native tissues. Notably, 3D bioprinting[8–10] is an advanced manufacturing platform that can provide an alternative source of 3D *in vitro* tissue models with high-throughput rates and reproducibility for toxicology studies. The 2D tissue models lack the complex 3D microenvironment[8–10] while the significant discrepancies in the detrimental effects of chemicals between humans and animal models lead to the demand for alternative *in vitro* models. Furthermore, 3D bioprinting has emerged as an advanced manufacturing platform for the fabrication of several tissues and/or organs such as the skin,[11,12] heart tissue,[13,14] bone,[15] liver,[16] tubular tissues[17] and cartilage.[18] Overall, 3D bioprinting offers radical solutions for the prevailing biomedical and healthcare problems.

There are two main printing approaches, namely the drop-on-demand (DOD) printing[19–21] (microvalve-based, inkjet-based and laser-based) and continuous printing[22,23] (extrusion-based). The DOD printing approach has several advantages over the continuous printing approach such as its highly precise control over the deposition pattern and material volume at pre-defined positions that facilitate the fabrication of spatially heterogeneous 3D bioengineered constructs with precise deposition of different types of cells and biomaterials.[24] It is highly challenging to create heterogeneity in such a subtle manner using the continuous printing approach. Major progress in the bioprinting field was observed over the last decade; the demand for improved bioprinting systems has spurred the development of more advanced printing systems for enhanced printing accuracy, consistency and reliability.[25] Particularly, the microvalve-based DOD bioprinting system has attracted tremendous attention for numerous applications such as high-throughput drug screening for toxicology studies, fundamental cell biology research, fabrication of *in vitro* tissue models and even *in situ* bioprinting of cells and extracellular matrixes for wound regeneration.[26–36] This article presents a comprehensive yet succinct review of a microvalve-based bioprinting system and performs a comparative evaluation of the microvalve-based DOD bioprinting system *versus* the other DOD bioprinting systems. We also provide an in-depth analysis of important considerations (system parameters, bio-ink properties and cellular components) during the printing process,

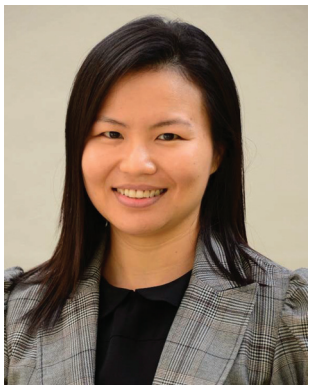

Wai Yee Yeong

Dr Wai Yee Yeong is an Assistant Professor in the School of Mechanical and Aerospace Engineering (MAE) at Nanyang Technological University, Singapore. Her main research interest is in Additive Manufacturing (AM), 3D printing, bioprinting, and the translation of the advanced technologies for industrial applications.

May Win Naing

*Dr May Win Naing heads the Bio-Manufacturing Programme (BMP) at the Singapore Institute of Manufacturing Technology, Agency for Science, Technology & Research (A*STAR), Singapore. Dr Naing obtained her first degree in Mechanical & Production Engineering from Nanyang Technological University, Singapore and pursued her PhD in the same university with a thesis focused on tissue engineering. Prior to joining A*STAR in 2013, she has worked at the EPSRC Centre for Manufacturing of Regenerative Medicine at Loughborough University, UK, and has also taken on R&D and Marketing roles in the medical device industry, specializing in spinal implants. Having worked in both academic and industry settings in Singapore and abroad, she is committed to the translation of technologies into the clinic and the market. Her research interest centers on scale-up manufacturing of biological products such as tissue scaffolds and cell therapies for applications in regenerative medicine, toxicity testing and consumer products. BMP's current studies focus on research and innovation of manufacturing platforms for processing of cells and materials for such applications.*

report the recent studies/applications using the microvalve-based bioprinting system and propose a future outlook on the DOD bioprinting system. We aim to present a timely review of an emerging bioprinting technology that should be of interest to the tissue engineering community with a reach towards the broader community interested in applying 3D bioprinting approaches for tissue engineering and regenerative medicine (TERM) applications.

Drop-on-demand (DOD) bioprinting systems

DOD bioprinting systems

There are currently many variations of bioprinting systems[37–40] available commercially; the DOD bioprinting systems are favourable over continuous bioprinting systems due to their ability to create complex 3D heterocellular constructs comprising multiple types of cells that are positioned relative to each other with a high degree of specificity and enhance its homology to native tissues and/or organs. We will discuss and evaluate the three main types of DOD bioprinting systems (microvalve-based, inkjet-based, and laser-based) (Fig. 1) in the following sections.

Microvalve-based bioprinting. A typical microvalve-based bioprinting system comprises a three-axis movable robotic platform and an array of multiple electromechanical microvalve print-heads. Each microvalve print-head is connected to an individual gas regulator that provides the pneumatic pressure (positive pressure) and the valve opening time (minimum 0.1 ms) which is controlled by the movement of both the plunger and the solenoid coil. The applied voltage pulse induces a magnetic field in the solenoid coil that opens the nozzle orifice by pulling the plunger up in an ascending motion. The bio-ink is deposited when the pneumatic pressure overcomes the fluid viscosity and surface tension at the opened orifice. The material deposition process is highly dependent on the nozzle diameter, the viscosity and surface tension of the bio-ink, the pneumatic pressure and the valve opening time.[41]

It offers controlled deposition of materials *via* a layer-by-layer fabrication approach; the key advantages of microvalve-based bioprinting are the synchronized ejection of biomaterials and cells from different print-heads, deposition of a thin material layer (1–2 μm thickness), precise cellular positioning with high viability greater than 86%[33] and high throughput printing (~1000 printed droplets per second).[41] However, it is only possible to print hydrogels within a limited range of viscosities (~1 to 200 mPa s) and cell concentrations of up to 10^6 cells per ml due to the clogging issues in the small nozzle orifice (100–250 μm).[34,41] The cells tend to sediment over time, affecting the overall cell homogeneity within the bio-inks.

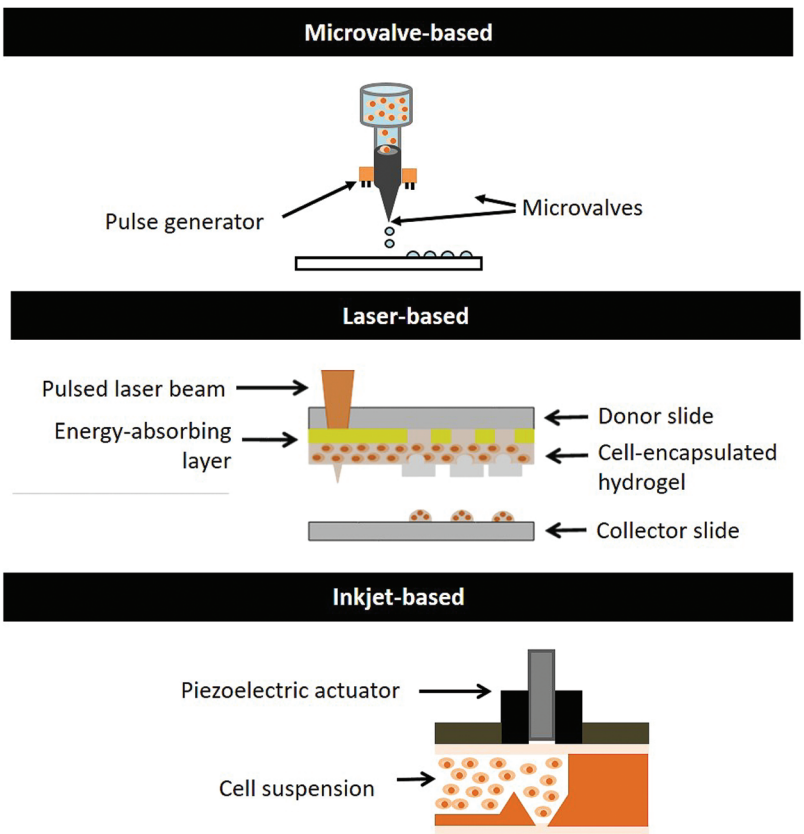

Fig. 1 Schematic drawing of different DOD bioprinting systems.

Inkjet-based bioprinting. Inkjet bioprinting manipulates bio-inks to facilitate the deposition of liquid droplets. It leverages the physical properties (density, viscosity and surface tension) of bio-inks for successful deposition of nano-liter droplets onto a receiving substrate. Inkjet bioprinting can be classified into two different categories: (i) continuous inkjet bioprinting and (ii) drop-on-demand (DOD) inkjet bioprinting. As the DOD inkjet bioprinting is more widely-utilized than the continuous inkjet bioprinting for tissue engineering applications, the authors have confined this review to only DOD inkjet bioprinting. DOD inkjet bioprinters comprise a single or multiple print-heads. Each print-head consists of a fluid reservoir and a varying number of nozzles. The surface tension at the nozzle orifice prevents the leakage of the bio-ink from the fluid reservoir.[42] There are many variations of DOD inkjet bioprinters; namely thermal, piezoelectric, electrostatic and electrohydrodynamic inkjet bioprinters. Generally, a droplet is ejected when the pressure pulses applied by using a thermal or a piezoelectric or an electrostatic actuator overcome the surface tension of the bio-ink at the nozzle orifice, whereas the electrohydrodynamic inkjet bioprinter utilizes the electrostatic stress between the metallic nozzle and the charged substrate to overcome the surface tension at the orifice under a sufficiently high voltage. The different mechanisms of these inkjet-based print-heads have been discussed in detail elsewhere.[19] The key advantages of inkjet-based bioprinting are its high printing resolution (20–60 μm) and low droplet volume (1–100 pL).[20] Nevertheless, it faces challenges in terms of its poor printing stability at high-throughput rates (>500 Hz),[43] low range of printable viscosities (3–30 mPa s),[44] clogging of the nozzle orifice due to cell sedimentation,[45] and potential cell desiccation during the printing process.[46]

Laser-based bioprinting. A laser-based system consists of a pulsed laser beam with a focusing device, a donor slide (with a layer of an energy-absorbing layer, followed by another layer of a cell-encapsulated hydrogel) and a collector slide facing the ribbon. It is a nozzle-free printing technique that eliminates the clogging issues and enables printing of high cellular density (>10^7 cells). A blade coater is used to form a homogeneous layer (~50 μm thickness) of a cell-laden hydrogel and a gap of 350–500 μm is maintained between the donor and collector slides.[47] The energy-absorbing layer first absorbs the laser energy; next the vaporized energy-absorbing layer induces a pressure which ejects the droplets of the cell-encapsulated hydrogel toward the collector slide. The printing resolution is highly dependent on the bio-ink viscosity, laser energy and pulse time.[48] The repetitive printing process facilitates the fabrication of a multi-layered construct with accurate positioning of cells and materials at pre-defined locations. The benefits of laser-based bioprinting include the use of high cellular density on the order of 1×10^8 cells per ml at high printing resolutions (~40 μm), a wider range of printing viscosities (1–300 mPa s) compared to other DOD bioprinting systems[49] and high cell survival rates (>90%).[47] Some shortcomings of the laser-based systems include slow throughput rates (~20 printed droplets per second),[47] non-uniform cell distribution of the coated cell-laden hydrogel at low cellular density,[48] fast drying of the thin cell-encapsulated hydrogel layer (~50 μm)[50] and the possible transfer of harmful residues from the energy-absorbing layer.[51] The printing output could be amplified by maximizing the laser pulse rate and increasing the number of laser beams. To address the problem of poor cell distribution in the ribbon, a higher cellular density (>10^8 cells per ml) is required to ensure that at least a single cell is contained in each printed droplet.[48] Furthermore, the use of a shock-absorbing polyimide membrane could mitigate the transfer of harmful metallic residues to the final printed products through mechanical deformation.[52]

A comparative evaluation of DOD bioprinting systems

As highlighted in the earlier section, the DOD printing approach has several advantages such as its good control over the deposition pattern and material volume at pre-defined positions. Furthermore, it offers high-throughput DOD bioprinting capabilities in a highly reproducible manner, which is highly desirable in high-throughput screening applications. It is highly challenging to achieve such similar results using the continuous printing approach. Particularly, DOD bioprinting has great clinical translational potential in tissue reconstruction. It can be utilized for *in situ* bioprinting of tissue defects (such as skin burns, deep wounds[11] or even craniofacial reconstruction[53]) *via* deposition of biologics in a non-contact manner to cover the wound site (usually non-planar). In the following sections, we provide an in-depth analysis of the different DOD bioprinting systems and present them in Table 1.

Ease of operation. For inkjet-based bioprinting, the droplet size and deposition rate are closely related to the fluid's viscosity and surface tension. The droplet deposition process can be controlled by varying the vibration frequency (Hz) and the driving voltage waveform. In order to achieve single droplet dispensing in the inkjet-based bioprinting system, there is an optimal range of pulse width ($p_{w,max}$ and $p_{w,min}$) for each corresponding pulse amplitude (p_a). No droplet is formed before $p_{w,min}$, whereas satellite droplets are generated above $p_{w,max}$.[43] Optimization of the pulse width and amplitude is necessary to ensure stable ejection of discrete droplets (Fig. 2).[20,43] The profound relationship and cursory knowledge of these parameters in actuating the piezoelectric printhead compound the difficulty of establishing stable droplets. Hence, determining the optimal dispensing conditions for each specific type of bio-ink is time-consuming.[43] For laser-based bioprinting, a 'ribbon' must be prepared prior to bioprinting. A layer of the energy-absorbing layer (~60 nm) is first coated on the donor slide, followed by manually-coating another layer of the cell-encapsulated hydrogel over the previous layer using a blade-coater. It is important to ensure a homogeneous cell-hydrogel layer (cell homogeneity and constant layer thickness). Furthermore, the preparation of multiple 'ribbons' is required (one ribbon for each specific type of cell) for the fabrication of heterogeneous cellular constructs. For microvalve-based bioprinting, the dispensing process is

Table 1 Performance comparison between different DOD bioprinting systems

	Microvalve-based	Inkjet-based	Laser-based
Working principle	Solenoid coil pneumatic pressure	Thermal/piezoelectric/electrostatic actuator	Laser source
Ease of operation	Simple printing mechanism	Complex printing mechanism	Easy printing mechanism
	Simple sample-loading	Simple sample-loading	Manual coating of a cell-hydrogel layer
Nozzle size	100–250 μm (ref. 34, 35, 41 and 43)	15–200 μm (ref. 19 and 43)	—
Highest printable resolution	1.5–2.5× nozzle size (~150 μm)[43]	1.2–2× nozzle size (~20 μm)[20,43]	Laser beam spot size (~40 μm)[48,55]
Viscosity	1–70 mPas (ref. 41 and 43)	3–30 mPa s (ref. 20)	1–300 mPa s (ref. 49)
Throughput rates	Up to 1000 Hz (ref. 41)	Up to 500 Hz (ref. 43)	Up to 20 Hz (ref. 47 and 55)
Cellular density	Up to 10^6 cells per ml (ref. 34 and 41)	Up to 10^6 cells per ml (ref. 60 and 61)	Up to 10^8 cells per ml (ref. 48)
Cellular viability	>80%[33]	>70%[59–61]	>90%[47]
Advantages	Easy operation	High printable resolution	Easy operation
	Reliable system for high-throughput printing		Wide range of printable viscosity
	Wide range of printable viscosity		High cell viability
Challenges	Cell sedimentation[45]	Cell sedimentation[45]	Difficult to incorporate multiple types of biologics[19]
	High shear stress experienced by cells[104]	Potential cell desiccation[46]	Non-uniform 'ribbon' thickness[47]
		Droplet instability at high printing frequencies[43]	Poor cell homogeneity of the coated 'ribbon' at low cellular density[48]
		High shear stress experienced by cells[104]	Fast drying of the 'ribbon' layer (50 μm)[50]
			Potential transfer of cytotoxic materials[51]

controlled by the valve opening time (VOT) and the printing pressure. Generally, a combination of a longer VOT and higher printing pressure is required to dispense more viscous fluids.[41,43] It is also important to note that a minimum printing pressure is required (~0.2 bar for water) to dispense the fluid. Nevertheless, additional pressure will not contribute to droplet generation once the fluid exceeds the range of printability. Overall, the microvalve-based bioprinting is a simple, user-friendly system that has an easy sample-loading procedure and does not require much trouble-shooting.[43]

Printable viscosities. Next, we compiled and analyzed the range of printable viscosities (determine the range of biologics that can be printed using the printing systems). Both the nozzle-based DOD bioprinting systems have a narrower printable range of viscosities (microvalve-based: 1–70 mPa s (ref. 41 and 43) and inkjet-based: 3–30 mPa s (ref. 20)) compared to the nozzle-free laser-based bioprinting system (1–300 mPa s (ref. 49)). The additional pneumatic pressure in the microvalve-based bioprinting system facilitates the deposition of more viscous bio-inks compared to the inkjet-based bioprinting system.[41] A longer valve-opening time and pressure is required to eject more viscous bio-inks for the microvalve-based bioprinting system, whereas a higher pulse amplitude is required for printing more viscous bio-inks.[43] Furthermore, it was shown that excessive pressure (in microvalve-based) or pulse amplitude (in inkjet-based) would generate undesired satellite droplets during the printing process.[43] Although the microvalve-based bioprinting system is capable of printing more viscous bio-inks (up to 200 mPa s), slow filament elongation (Fig. 2) was observed in the more viscous bio-inks (>70 mPa s).[43,54] In contrast to the nozzle-based DOD bioprinting systems, an increase in the bio-ink's viscosity (laser-based bioprinting) would require a higher laser energy for bio-ink deposition (resulting in a smaller droplet diameter for the same laser energy).[48]

Printing speed. The deposition speed of the printing system is critical for large-scale biomanufacturing and high-throughput screening applications. The inkjet-based bioprinting has the highest throughput rates of up to 30 kHz,[20] followed by the microvalve-based bioprinting (up to 1 kHz (ref. 41)) and lastly the laser-based bioprinting (20 Hz).[47,55] Although the inkjet-based bioprinter has the capability to achieve such a high-throughput rate, droplet instability was observed at high frequencies (>500 Hz) due to pressure fluctuations within the inkjet print-head.[43] In contrast, there is no droplet instability issue in the microvalve-based bioprinting at the optimal printing parameters, making it a more reliable bioprinting system for high-throughput bioprinting (up to 1 kHz).[41,43]

Printing resolution. Both the microvalve-based and inkjet-based bioprinter have nozzle sizes of 100–250 μm and diameters of 15–200 μm, respectively, whereas the laser-based bioprinting system is a nozzle-free bioprinting system. A study[43] has demonstrated that the nozzle size is the most significant parameter that influences the printing resolution. The printing resolution from the microvalve-based and inkjet-based print-head

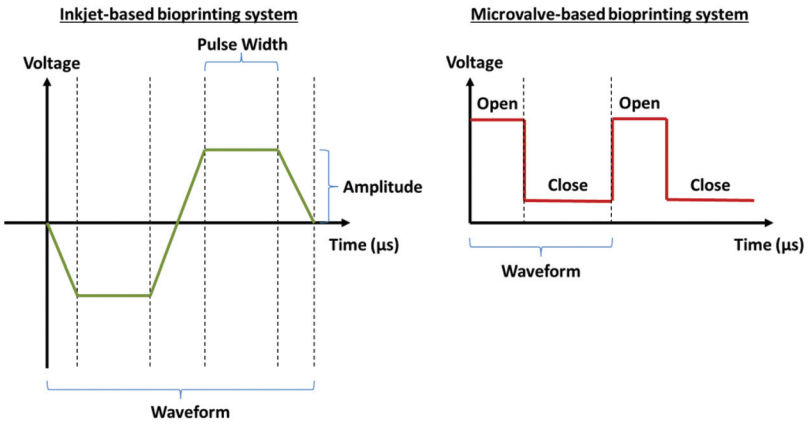

Fig. 2 Dispensing mechanisms for (left) the inkjet-based system and (right) the microvalve-based system.

(similar nozzle size) is approximately 1.5–2.5 times and 1.2–2 times the nozzle size respectively. This is due to the higher pushing force from the pneumatic pressure in the microvalve-based bioprinting that resulted in a slightly lower printing resolution compared to inkjet-based bioprinting.[43] In contrast, the printing resolution of the laser-based bioprinting system is highly dependent on the laser pulse profile (*i.e.* wavelength, pulse duration, beam energy and focus diameter) and bio-ink properties (thickness, surface tension and viscosity of the 'ribbon').[49] Overall, the inkjet-based bioprinting system has the highest printing resolution (~20 μm (ref. 20 and 43)) compared to other systems (laser-based: ~40 μm (ref. 48 and 55) and microvalve-based: ~150 μm (ref. 43)). Nevertheless, some complications to achieving such high printing resolution include the use of an extremely small nozzle orifice that induces higher shear stress to the viable cells,[56] a trade-off between the high printing resolution and scalability of the printed constructs[57] and lastly potential desiccation of the printed cells[46,58] due to the higher surface area to volume ratio of pico-liter sized droplets.

Cell viability. The living cells are an important consideration in bioprinting; both the microvalve-based and inkjet-based bioprinting facilitate printing up to 10^6 cells per ml with high cellular viabilities (microvalve-based: >80%,[33] inkjet-based: >70%[59–61]), whereas the laser-based bioprinting enables the printing of extremely high cellular densities (up to 10^8 cells per ml) with exceptionally high viability (>90%[47]). However, some of the challenges in laser-based bioprinting include difficulties to incorporate multiple types of biologics within the same 'ribbon',[19] non-uniform 'ribbon' thickness,[47] poor cell homogeneity of the coated 'ribbon' at low cellular density,[48] fast drying of the 'ribbon' layer (50 μm)[50] and potential transfer of cytotoxic materials[51] during the bioprinting process. In contrast, both microvalve-based and inkjet-based bioprinting experienced cell sedimentation[45] (gravitational force acting on the cells). Hence, there is a need to modify the bio-inks to mitigate the sedimentation effect and preserve high cellular viabilities while maintaining the bio-inks within the printable range of viscosities.[45]

Each printing system has its own advantages and limitations over the others in specific fabrication tasks. Both microvalve-based and inkjet-based bioprinting are superior over laser-based bioprinting in terms of fabrication of spatially heterogeneous 3D bioengineered constructs with precise deposition of different types of cells[19] and higher fabrication speed.[20,41] Particularly, the ability to create such spatially heterogeneous 3D constructs is the key advantage of 3D bioprinting over conventional tissue engineering approaches. As highlighted earlier, the microvalve-based bioprinting is a more reliable system for high-throughput printing (1 kHz) compared to the inkjet-based bioprinting (droplet instability issue at high frequencies of >500 Hz).[43] Furthermore, its wider range of printable viscosities would translate to broader bioprinting applications using microvalve-based bioprinting. Although the inkjet-based bioprinting can achieve the highest printable resolution *via* the use of an extremely small nozzle orifice (~15 μm diameter), it induces significantly higher shear stress to the viable mammalian cells (~20 μm diameter)[56] and it is reasonable to expect potential desiccation of the printed cells[46] due to the higher surface area to volume ratio of the pico-liter sized droplets. Overall, the microvalve-based bioprinting is a more reliable bioprinting system that facilitates precise control over the deposition of multiple types of cells and biomaterials with high cellular viabilities (>80%), high-throughput rates (up to 1 kHz) and with a moderate printing resolution (~150 μm).

Operation considerations for microvalve-based bioprinting

System considerations

Valve opening time. The valve opening time (VOT), printing pressure and the nozzle size are critical system parameters that determine droplet formation in a microvalve-based bioprinting system. As the viscosity increases, a longer VOT is necessary to generate the bio-ink droplet. However, a VOT that is higher than VOT_{max} will induce the formation of satellite

droplets.[43] Hence, there is an optimal range of VOT values [VOT_{min}, VOT_{max}] to achieve single droplet dispensing for each specific bio-ink.[43]

Printing pressure. A minimum printing pressure is required to provide an adequate force for droplet generation and this p_{min} increases with increasing fluid viscosity. When the pressure is below the minimum printing pressure, a huge droplet will start to accumulate on the nozzle orifice due to the insufficient force to overcome the surface tension of the fluid. In contrast, excessive printing pressure would result in the formation of satellite droplets. The printing pressure has a huge influence on the cellular behaviour; it was reported that cells that were exposed to an optimal printing pressure of less than 0.5 bar will not exhibit any detrimental short-term or long-term impairments.[56]

Nozzle size. It was reported that a variation in the nozzle size is a more effective approach to tune the droplet diameter, whereas a variation in printing pressure (0.15–0.4 bar) does not result in a significant change in the droplet diameter.[43] Although the smallest nozzle diameter provides the highest printing resolution, it also has the narrowest range of optimal VOT values.[43] Hence, more time and experience is required to optimize the process for high resolution microvalve-based printing.

Bio-ink considerations

Physical properties of bio-inks. The DOD microvalve-based printing deposits precise quantities of functional bio-inks at high throughput rates (up to the kHz range) in the form of droplets (nL–μL); the droplet volume is controlled by varying the printing pressure and valve opening time (0.1 ms and beyond). The range of printable hydrogels for DOD bioprinting systems has been covered extensively elsewhere,[19,62] hence we will instead discuss the critical aspects of the bio-inks. The microvalve-based bioprinting system is an advanced manufacturing platform that facilitates the precise deposition of bio-inks with moderate viscosities (up to 70 mPa s),[41,43] and the four key parameters that influence the printability include viscosity, density and surface tension of the printable bio-inks and the radius of the printing orifice.[54] An approximate solution to the Navier–Stokes equations for printability of the bio-inks can be represented by the Reynolds number (N_{Re}: the ratio of inertial to viscous forces) and the Weber number (N_{We}: a balance between the inertial and capillary forces).[63]

$$N_{Re} = \frac{vr\rho}{\eta} \quad (1)$$

$$N_{We} = \frac{v^2 r\rho}{\gamma} \quad (2)$$

$$Z = \frac{N_{Re}}{(N_{We})^{1/2}} = \frac{(r\rho\gamma)^{1/2}}{\eta} \quad (3)$$

where v, ρ, η and γ are the mean droplet velocity, density, viscosity and surface tension of the bio-inks, respectively, and r is the radius of the orifice. The dimensionless number Z, an inverse of the Ohnesorge number (Oh), is the ratio between the Reynolds number (N_{Re}) and a square root of the Weber number (N_{We}), and is not affected by the bio-ink velocity.

The printability of the bio-inks is governed by the Z values ($4 \leq Z \leq 12$); the lower limit of Z is governed by the maximum printable bio-ink viscosity whereas the upper limit is determined by the point at which the satellite droplets are formed[54] (Fig. 3). During the printing process, bio-inks with low

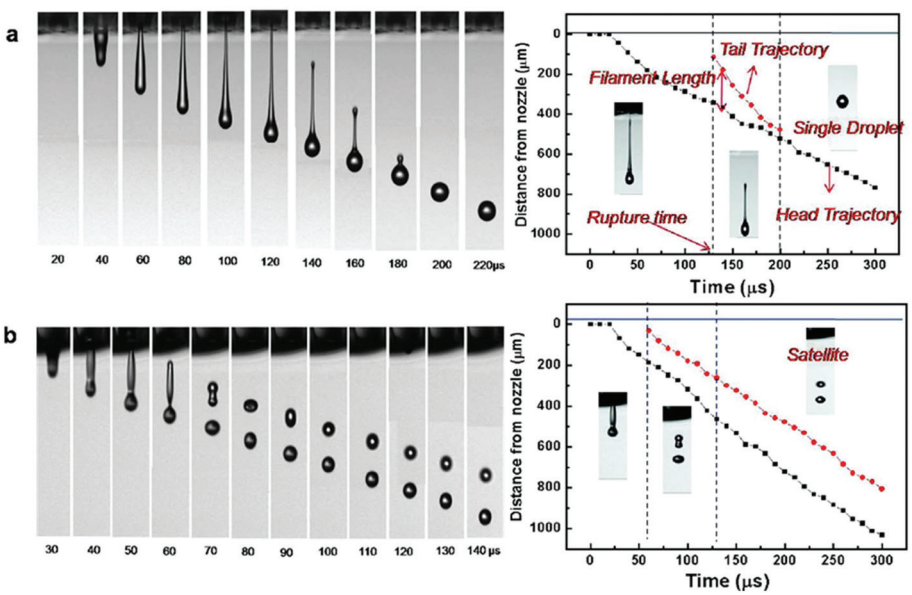

Fig. 3 (Left) Representative photo sequence of droplet formation and (right) representative trajectories of the ejected droplets as a function of the elapsed time for bio-inks with varying values of Z: (a) Z = 2.17; (b) Z = 17.32. "Reprinted (adapted) with permission from ref. 45. Copyright (2009) American Chemical Society".

Z values ranging from 2 to 4 experience slower filament elongation. This leads to a longer rupture time and results in a slower droplet velocity.[54] In contrast, bio-inks with high *Z* values of above 14 experience more rapid filament elongation and rupture. The resultant satellite droplets during the printing process are unable to merge with the primary droplet even before reaching the substrate surface, hence resulting in poor printability (deposition of tiny satellite droplets around the primary droplet on the substrate surface). Therefore, it is imperative to tune the physical properties (density, surface tension and viscosity) of the bio-inks within a suitable range of *Z* values to achieve good printability at high-throughput rates.

Chemical properties of bio-inks. The bio-inks that are commonly used in the bioprinting systems can be classified as physical or chemical hydrogels based on the formation mechanism.[62] The physical hydrogel is dynamic as the network formation is dependent on the non-covalent interactions (such as hydrogen bonds, ionic bonds, complex formation or π–π stacking) between the building units. Furthermore, the physical hydrogels are highly suitable for bioprinting processes due to the dynamic and reversible nature of the cross-linking mechanisms and their excellent bioactivity.[64] Some examples of physical hydrogels include proteins (collagen, fibrin, gelatin and silk) and polysaccharides (alginate, agarose and chitosan). However, these physical hydrogels possess low mechanical strength and stability.

In contrast, the covalent bonds found in the chemical hydrogels resulted in a highly stable but less dynamic network. The various cytocompatible chemical cross-linking mechanisms for cell-encapsulated hydrogels include polymerization, redox reactions, enzyme-driven reactions and classical organic reactions (*e.g.*, Michael addition and click chemistry).[62] It is important that the formulation remains printable throughout the printing process and rapid chemical cross-linking should occur immediately after printing to ensure high shape fidelity of the printed constructs.

Bio-ink–substrate interactions. Upon impact, the printed bio-inks divert outward and expand radially along the substrate surface to form a spherical droplet. The impact of the printed droplets on the substrate surface (maximum droplet spread and rebound) is mainly influenced by the bio-ink viscosity, substrate hydrophilicity and impact velocity.[65] The energy dissipation during the droplet impact increases with increasing bio-ink viscosity, thus a droplet with a higher viscosity produces a smaller droplet spread upon impact and has less available energy for droplet rebound. A similar phenomenon is observed on a more hydrophilic substrate surface; the area of the liquid–substrate contact during rebound decreases slowly on a more hydrophilic substrate indicating higher energy dissipation on a more hydrophilic surface.[65] Lastly, a higher impact velocity leads to an increase in the maximum energy available for droplet rebound. As a result, the droplet rebounds higher with increasing impact velocity.[65] A good understanding of the printing process (working principle, droplet generation from the nozzle and droplet impact on the substrate surface) allows us to control the printing resolution and accuracy of the bioprinted droplets.

Cellular considerations

Cell sources for bioprinting. Most of the published bioprinting studies utilized cell lines that are very robust and have substantial proliferation capacity for proof-of-concept studies.[33,34] The cells used for bioprinting applications must be robust enough to survive the bioprinting process (withstand the high shear stress, the presence of cross-linkers or even non-physiological pH). It is also critical for the choice of cells to be able to expand into sufficient numbers for printing. The different types of printed cells include fibroblasts,[34–36] keratinocytes,[34,36] HEK-293,[28] astrocytes,[32] neurocytes,[32] HUVECs,[33] human alveolar epithelial cells,[33] and even stem cells.[26,27,29–31] Stem cells are also attractive cell sources due to their potential to proliferate and generate multiple functional tissue-specific cell phenotypes. The stem cells not only have high proliferation and differentiation capacity but they can also be isolated and propagated easily with the established protocols.[66–68] The capacity of stem cells to generate a large number of cells indicates the potential of these cells for bioprinting applications. Nevertheless, it is still critical to conduct more preclinical trials to evaluate the potential risks of malignant teratoma formation and long-term adverse effects of these stem cells.

Maximum printable cell concentration. Cells are usually encapsulated within a delivery matrix such as the culture media or hydrogels; the cell concentration within the bio-ink determines the number of printed cells in each droplet. Here, we discuss and analyze how the changes in the cell concentration affect the properties of the bio-inks and the different parameters that limit the maximum printable cell concentration. As highlighted in the previous section, the physical properties of the bio-inks (surface tension and viscosity) have a great influence on the printability. A higher cell concentration increases the bio-ink viscosity due to the distortion of the fluid flow and the friction exerted by the bio-ink flow at the cell surface (increased energy dissipation).[69] The increase in cell concentration also reduces the surface tension of the bio-ink as the total free energy of the bio-ink decreases (more cells are adsorbed to the interface).[69] Overall, an increase in cell concentration results in a lower *Z* value and it is critical to ensure that the resultant bio-ink still remains within the printable range of *Z* values (Fig. 4). Another important factor that determines the optimal printable cell concentration is the nozzle size. Cell sedimentation is a prevalent issue in most bioprinting systems; the gravitational forces act upon the suspended cells in the bio-ink and cause the accumulation of mammalian cells (~20 μm) at the nozzle orifice over time (Fig. 4). It was reported in a study that a cell concentration (higher than 3 million cells per ml) induced clogging issues in the nozzle with a diameter of 150 μm.[41] Hence, an optimal cell concentration (typically within the range of 1–3 million cells per ml) is highly dependent on the *Z* value of the resultant bio-inks and the nozzle orifice diameter.

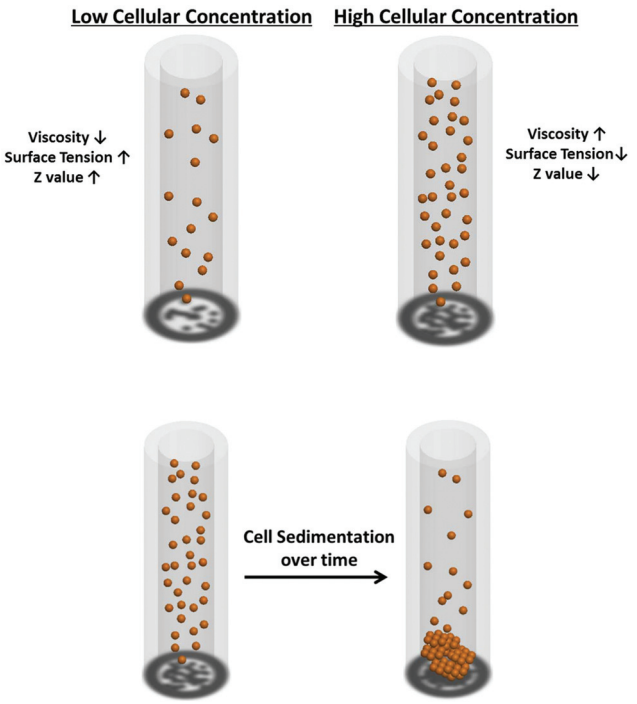

Fig. 4 (Top) Influence of cellular concentration on the physical properties of the resultant bio-inks, (bottom) cell sedimentation over time.

Applications

With a better understanding of different DOD bioprinting systems and the key considerations for microvalve-based bioprinting (with regard to system parameters, bio-ink properties and cellular components), we next highlight the use of microvalve-based bioprinting (Fig. 5) for numerous applications (Table 2).

High-throughput screening for toxicology studies

Although micro-engineering approaches such as microfluidic-based manipulation, soft-lithography and surface patterning[70] have been utilized for high-throughput screening, the DOD bioprinting system offers several advantages that include high repeatability and high-throughput rates. The microvalve-based DOD bioprinting has been utilized in many studies to conduct biological studies through 3D-array patterning.[30,71–74] The enabling technologies that facilitate rapid isolation of viable single cells from heterogeneous solutions have contributed significantly to the field of medical genomics; the understanding of single-cell level functional genomics for stem cell characterization has become increasingly important.[75] The microvalve-based bioprinting approach eliminated the need for additional cell isolation steps in conventional fluorescence-activated cell sorting (FACS) and microfluidic set-ups.[76] The cellular densities and printing parameters were tuned to optimize the number of droplets containing single cells; next RNA extraction was conducted within the nanoliter-scale droplets containing the targeted cells for genomic analysis. Furthermore, nanomaterials (different types and concentrations) can be deposited alongside the cells to provide valuable insights into the potential risks and health impacts associated with nanomaterial exposure.

Fundamental cell biology research

The extracellular microenvironment has a huge influence on cellular behaviour;[77,78] numerous studies are currently focused on the development of biomaterials that provide optimal cellular substrates.[79,80] A pioneering study reported the high-throughput nanoliter-scale synthesis of arrayed biomaterials (576 different combinations of 25 different acrylate-based polymers) followed by seeding of human embryoid bodies (EBs) onto the arrays for large-scale cellular–biomaterial interactions; the study elucidated a plethora of unforeseen material effects that provide unprecedented control over human embryonic stem cell (hESC) behaviour.[26] Another study presented an extracellular matrix (ECM) microarray platform for the culture of seeded mouse embryonic stem cells (mESCs) on different combinatorial matrix mixtures (collagen I, collagen III, collagen IV, laminin and fibronectin);[27] this approach enables the facile identification of the synergistic effects of different combinations of ECMs on cellular differentiation at high resolution (nanolitre-scale) in a highly repeatable manner.

Another interesting application is to fabricate uniform-sized tissue spheroids using the microvalve-based bioprinting system.[31] Embryonic stem cells (ESCs) are pluripotent cells with multi-lineage differentiation potential; this unique feature of pluripotency makes ESCs an ideal cell source for tissue regeneration applications.[81,82] The embryoid bodies (EBs) mimic the early stages of embryogenesis and they play critical roles in *in vitro* ESC differentiation. Various methods have been utilized to form EBs;[83–85] but challenges persist to form EBs with controlled size and uniformity in a highly-reproducible manner. The microvalve-based bioprinting approach has been utilized for the formation of controllable, uniform-sized EBs by integrating bioprinting technologies with the existing hanging-drop methods.[31] The EB size and uniformity are important factors that affect the phenotypic expression of embryonic stem cells (ESCs).[86,87] The number of cells encapsulated within each printed droplet can be controlled by manipulating the droplet volume and cellular concentration to fabricate the resultant cellular aggregates with controllable and repeatable sizes (0.25–0.6 mm).

Fabrication of *in vitro* 3D tissue models

Traditional tissue engineering approaches involved the seeding of cells over prefabricated scaffolds, which resulted in a random and non-uniform distribution of cells that does not truly reflect the sophisticated hierarchical organization of native tissues.[88,89] 3D bioprinting enables precise control over the spatial deposition of multiple types of biomaterials and cells to improve the homology to native tissues and/or organs; the ability to recapitulate the complexity of native tissues/

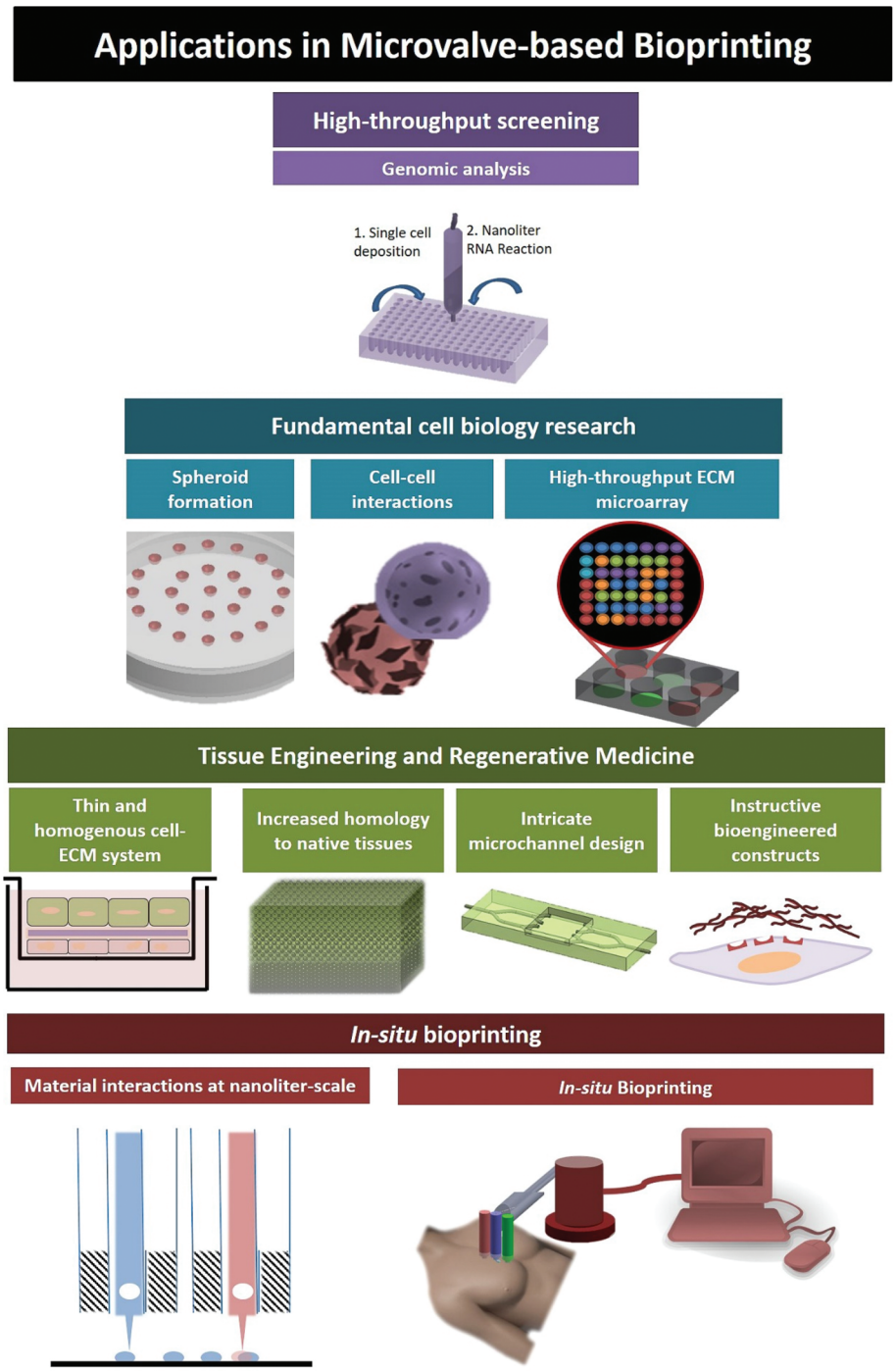

Fig. 5 Applications of microvalve-based bioprinting; (A) high-throughput screening, (B) fundamental cell biology research, (C) fabrication of *in vitro* tissue models, (D) *in situ* bioprinting.

organs using AM approaches is highly attractive for the fabrication of functional tissue-engineered constructs.

Previous studies have demonstrated the ability to fabricate 3D constructs from 2D hydrogel droplets using the microvalve-based printing approach;[34,35,41,90] the hydrogel droplets and cells were deposited simultaneously *via* epitaxial layering to fabricate 3D tissue-engineered constructs. Furthermore, complex hollow 3D structures consisting of fugitive support materials and hydrogels can also be printed using the microvalve-based bioprinter.[56]

Biological *in vitro* 3D models such as smooth muscle cell patches, air–blood barrier models and skin tissue models have been bioprinted using microvalve-based systems.[33,34,90,91] Microvalve-based bioprinting facilitated the homogeneous patterning of cells on the thin layers of bioprinted ECMs at controlled proximity; the printed cells formed a thin

Table 2 Microvalve-based bioprinting for numerous applications

Applications	Materials and cells	Resolution		Advantage or outcome	Ref
		Diameter	Volume		
High-throughput screening					
RNA analysis	Mouse embryonic stem cell suspension	250 μm	—	Array patterning Single cell droplet generation for RNA analysis	30
Fundamental cell biology research					
ECM micro-arrays	Acrylate-based polymers Human embryoid bodies (EBs)	—	~nl	Large-scale cell–ECM interactions	26
ECM micro-arrays	Combinatorial matrix mixtures (collagen I, III, IV, laminin and fibronectin) Mouse embryonic stem cells (mESCs)	500 μm	—	Large-scale cell–ECM interactions	27
Formation of tissue spheroids	HEK-293 cell suspension Human embryonic stem cell suspension	250–600 μm	4–120 nl	Controllable, uniform-sized EBs in a highly reproducible manner	31
Cell–cell interactions	Collagen type I precursor Astrocytes from embryonic rats Neurocytes from embryonic rats	— — —	8 nl 11 nl 11 nl	Optimal inter-cellular distance to regulate neurite outgrowth and astrocyte morphology	32
***In situ* transplantation of tissues**					
In situ bioprinting	Fibrin/collagen type I matrix Keratinocytes Fibroblasts	— — —	— — —	Direct cell delivery for wound healing Complete re-epithelialization of large wounds (10 cm × 10 cm) after 8 weeks	36
Rapid hydrogel formation for *in situ* bioprinting	Complementary pairs of DNA-conjugated hydrogels AtT-20 anterior pituitary cells HEK-293 cells	500 μm	~60 nl	Rapid hydrogel formation at the nanoliter-scale level (within one second)	28
Tissue engineering and regenerative medicine (TERM)					
3D scaffold for neural cell migration studies	Collagen type 1 precursor Fibrinogen, VEGF and aprotinin Thrombin, heparin, VEGF and calcium chloride Murine neural stem cell C17.2	500 μm — — 700 μm	— — — 11 nl	Fabrication of instructive bioengineered constructs	29
In vitro air–blood barrier model	Matrigel Human alveolar epithelial cell A549 EA.hy926 (fused HUVEC with A549)	— — —	— — —	Thin and homogeneous bioprinted ECM layers (1–2 μm) for enhanced cellular interactions	33
In vitro skin model	Collagen type I Human keratinocytes (HaCaT) Human neonatal foreskin-derived fibroblasts (HFF-1)	500 μm 500 μm 500 μm	52 nl 28 nl 28 nl	Uniform gelation of collagen hydrogels Controlled cellular densities within 3D bioprinted constructs	34
Fabrication of micro-channels within 3D bioprinted constructs	Collagen type I Gelatin type A porcine skin Primary human dermal fibroblasts	400 μm 200 μm —	— — —	Enhanced cellular viabilities within thick 3D constructs	35

homogeneous cellular layer whereas the manually-seeded cells formed discrete multi-layered cellular clusters. This thin layer of bioprinted ECM (1–2 μm), unlike the thick ECM layer (20–30 μm) in the manual approach, facilitated enhanced cell–cell interactions that induced higher structural and functional resemblance to the native air–blood barrier.[33] Furthermore, the microvalve-based bioprinting approach was utilized to achieve representative cellular densities within the different regions of the bioengineered 3D construct to improve the homology to native tissues and/or organs.[34] It was also reported that the bioprinted constructs (6 × 6 × 1.2 mm) formed by repeated deposition of the collagen precursor (each droplet ~52 nL) retained their shape and dimensions whereas the conventional manually-seeded constructs underwent significant changes in shape and dimensions during culture.[34] The bioprinting approach facilitated nanoliter-scale deposition of biomaterials that resulted in uniform gelation of hydrogels compared to the conventional manual mixing approach.[34]

Furthermore, the precise control over cellular deposition by the DOD microvalve-based bioprinting facilitates the fabrication of co-culture models. The cells are spatially patterned in their 3D microenvironment to facilitate an intricately orchestrated exchange of stimuli that influence their cellular behaviour;[92] the precise control over the patterning of multiple types of cells is critical for eliciting critical cell–cell interactions. It has been demonstrated that an optimal patterning distance is required to regulate the neurite outgrowth and morphology of neurons (150 μm) and astrocytes (400 μm) respectively.[32] The spatial positioning of these patterned neural cells at optimal proximity recapitulated important cell–cell interactions for potential organoid construction.

Cells encapsulated within the 3D bioprinted tissue-engineered constructs are required to undergo a maturation process prior to implantation; adequate perfusion of growth factors, oxygen and other nutrients to the cells is necessary during the maturation process.[93–95] The microvalve-based bioprinting approach has been used to design and fabricate intricate channels within the 3D bioprinted constructs; micro-channels were printed within a 3D collagen scaffold that enabled medium perfusion throughout the bioprinted construct.[35] Gelatin was used as a sacrificial material to fabricate microchannels (400 μm width and 100 μm height) that were subsequently removed to create perfusable channels. This enhanced the cellular viability within the 3D constructs and holds great potential for the fabrication of thick bioengineered constructs with complex vasculature-like networks.

In situ bioprinting

The advent of *in situ* bioprinting could revolutionize future surgical practice as it can be used to directly deposit bio-inks at the defective site in the living body *via* the aid of highly automated robotic arms in a non-contact manner.[96] As such, the human body functions as an "*in vivo* bioreactor" to facilitate the maturation of printed constructs in the most ideal biological microenvironment.

The human skin, being the largest and most easily accessible organ in the body, has huge potential for *in situ* bioprinting applications, especially potentially useful in burn injuries. Burn injuries are a common source of morbidity and mortality;[97] the patient survival is directly proportional to the rate of wound closure. A feasibility study on *in situ* bioprinting was conducted on full-thickness large wounds (10 cm × 10 cm) of nude mice using a microvalve-based bioprinting system.[36] It was reported that complete re-epithelialization of the large wound was achieved after 8 weeks. Another study reported the *in situ* printing of amniotic fluid-derived stem cells (AFSCs) and bone marrow-derived mesenchymal stem cells (MSCs) over full-thickness wounds on the backs of mice.[98] Multiple layers of a fibrin–collagen hydrogel were used as the carrier to deliver the stem cells directly to the wound sites. The AFSCs secreted trophic factors that expedited the rate of wound closure in full-thickness wounds and increased neovascularization was observed.

Another work reported the rapid hybridization of complementary DNA motifs to form mechanically strong supramolecular polypeptide–DNA hydrogels under physiological conditions.[28] The fast diffusion between the nanoliter-scale printed DNA droplets induced a much rapid hydrogel formation (within one second) compared to the manual mixing of a bulk DNA-based hydrogel (within several seconds). The printed DNA-based hydrogel does not exhibit any obvious shrinkage or swelling behavior, making it an attractive choice of a printable biomaterial for potential *in situ* bioprinting applications. Despite the significant advances in the pilot studies on *in situ* bioprinting of tissues/organs, further optimization of the bioprinting techniques is essential to achieve functional *in situ* bioprinting for immediate repair of wounds in humans.

Future outlook

Improving cell homogeneity in bio-inks

Cell sedimentation was shown to affect the printing output consistency over time;[99,100] which is a common problem in most of the existing bioprinting systems. This cell sedimentation effect can be mitigated by decreasing the sedimentation velocity, v, through neutral buoyancy of the cells and increasing the viscosity of the bio-inks within the printable Z range as discussed in the earlier section. The theoretical solution for sedimentation velocities was obtained using Stokes' law as[101]

$$v = \frac{(\rho_{\text{cell}} - \rho_{\text{bio-ink}})gD_{\text{cell}}{}^2}{18\eta} \quad (4)$$

where ρ_{cell}, $\rho_{\text{bio-ink}}$, g, D_{cell} and η are the density of the cell, density of the bio-ink, gravitational acceleration, diameter of the cell size and the viscosity of the bio-ink respectively. Although studies have been conducted to mitigate the cell sedimentation effect through neutral buoyancy,[45,100,102,103] another possible phenomenon such as cell adhesion on the interior surface of the printing cartridge affects the overall cell

homogeneity during the printing process. The issue of cell adhesion during the bioprinting process is yet to be thoroughly studied.

Printing-induced cell damage

Despite numerous studies conducted on DOD bioprinting, most of the prior studies focused on the droplet formation process (printability) and little emphasis is placed on the post-impact viability of the printed cells. A recent study reported that the phenotype and the proliferation potential of the cells can be retained when printed below the specific shear stress threshold (<5 kPa).[104] It was highlighted in another study that the droplet impact (substrate stiffness) has a more adverse effect than the shear stress during the printing process.[105] There is still an unmet need to fully comprehend the relationship between the droplet formation process and post-printing cell viability. Interestingly, the detrimental droplet impact on the substrate surface could be minimized by reducing the pressure (from ambient pressure to 0.3 atm) within the printing chamber.[106] The ejected droplet gently spreads on the substrate surface with no subsequent splashing under reduced atmospheric pressure (0.3 atm).[107] Furthermore, it is also critical to investigate the influence of temperature on cellular viabilities and damage during the printing process. The widespread applicability and future success of bioprinting technologies would benefit from the evaluation of cellular functions during and after bioprinting.

Bio-ink development

Furthermore, the progress in the bioprinting field is currently hindered by the limited choices of printable bio-inks;[108–112] the stringent requirements for the bio-inks include printability and biocompatible cross-linking mechanisms. Particularly, the dynamic reciprocity between a cell and its microenvironment is critical for recapitulating cell–biomaterial interactions.[92] Despite numerous reports on bioprinted cell-encapsulated constructs, inferior tissue formation and sparse cellular–biomaterial interactions are the foremost concerns. These materials cannot fully emulate the complexity of natural extracellular matrices (ECMs), which is necessary to guide tissue formation and recapitulate important cell–cell interactions. Recent studies on cells and ECMs isolated from specific tissues and organs highlighted the importance of tissue specificity for preserving critical cellular functions and phenotypes.[113–115] Although a decellularized extracellular matrix (dECM) is an attractive source of biomaterial,[116] incomplete removal of cellular remnants may induce potential pro-inflammatory responses.[117] A plausible solution is to reconstruct the unique ECM niche *via* patterning of the desired types of biomaterials at specific regions to emulate a biomimetic microenvironment that can better satisfy the natural niche for specific types of cells. Hence, the ability to emulate the biochemical and physical microenvironment with the controlled 3D spatial deposition of specific types of biomaterials and cells at high resolution and accuracy is critical towards achieving the goal of fabricating fully-functional bioengineered constructs.

Hybrid bioprinting

Hybrid bioprinting, through integrating other fabrication technologies with bioprinting, provides an attractive approach to fabricate 3D hierarchical constructs with macro, micro- and nano-scale features.[118,119] Surface topography plays an important role in influencing cellular behaviour;[120] microscale topographies can influence the shape and motility of cells[121] whereas the nanoscale topographies can alter differentiation and proliferation of stem cells.[122] The bioprinting approach has its limitations in creating such nanoscale structures that are critical in directing cellular differentiation. To address these limitations, bioprinting/electrospinning hybrid systems could be used to fabricate complex constructs with intricate nanoscale structures and deposit highly viable cells at predefined regions. It has been reported that the combination of bioprinting/electrospinning approaches[118] facilitated the hybrid printing of cartilage constructs with improved biological and mechanical properties. Furthermore, the manufacturing speed plays an important role in realizing the goal of fabricating large-scale tissues and/or organs. Different bioprinting techniques could be utilized simultaneously to complement each other; such as the combination of DOD bioprinting systems (precise deposition of nano-liter cellular droplets with high viability[33]) with the continuous extrusion-based bioprinting system (a high deposition and printing speed, which can facilitate scalability within a relatively short period of time[22]). The complementary bioprinting approaches (microvalve- and extrusion-based) could facilitate simultaneous drop-on-demand printing of highly viable cells at specific positions and continuous extrusion of hydrogel filaments respectively to fabricate large 3D spatially-heterogeneous cell-laden printed constructs at high-throughput rates.

Concluding remarks

It is becoming increasingly obvious that the automated robotic platform is emerging as an imperative tool for TERM. Particularly, the DOD microvalve-based bioprinting system provides a highly advanced manufacturing platform that facilitates precise control over the cellular and biomaterial deposition in a highly reproducible and reliable manner. The holistic in-depth understanding of the influence of system parameters, bio-ink properties and cellular components on the printing outcomes provides valuable insights into the formulation of novel bio-inks and design of improved bioprinting systems. Furthermore, we also present and highlight the significance of DOD microvalve-based bioprinting in the reported studies/applications such as high-throughput ECM microarrays, cellular manipulation, fabrication of complex instructive constructs and *in situ* bioprinting. Apart from the discussion of recent progress in the bioprinting field, we also inform the readers about the existing limitations and highlight promising

directions to transform microvalve-based bioprinting into an enabling technology that will potentially drive significant advances in the field of TERM.

Conflict of interest

The authors declare no conflict of interest.

Acknowledgements

The authors would like to thank the scholarship sponsorship by A*STAR Graduate Academy and funding support of the NTU Start-up Grant.

References

1 C. K. Chua, K. F. Leong and C. S. Lim, *Rapid prototyping: principles and applications*, World Scientific, 2010.
2 F. Guillemot, V. Mironov and M. Nakamura, *Biofabrication*, 2010, **2**, 010201.
3 C. K. Chua and W. Y. Yeong, *Bioprinting: principles and applications*, World Scientific, 2014.
4 F. P. Melchels, M. A. Domingos, T. J. Klein, J. Malda, P. J. Bartolo and D. W. Hutmacher, *Prog. Polym. Sci.*, 2012, **37**, 1079–1104.
5 B. Derby, *Science*, 2012, **338**, 921–926.
6 S. V. Murphy and A. Atala, *Nat. Biotechnol.*, 2014, **32**, 773–785.
7 J. M. Lee and W. Y. Yeong, *Adv. Healthcare Mater.*, 2016, **5**, 2856–2865.
8 S. Knowlton, A. Joshi, B. Yenilmez, I. T. Ozbolat, C. K. Chua, A. Khademhosseini and S. Tasoglu, *Int. J. Bioprinting*, 2016, **2**, 3–8.
9 S. Knowlton, S. Onal, C. H. Yu, J. J. Zhao and S. Tasoglu, *Trends Biotechnol.*, 2015, **33**, 504–513.
10 W. Peng, D. Unutmaz and I. T. Ozbolat, *Trends Biotechnol.*, 2016, **34**(9), 722–732.
11 W. L. Ng, S. Wang, W. Y. Yeong and M. W. Naing, *Trends Biotechnol.*, 2016, **34**, 689–699.
12 W. L. Ng, W. Y. Yeong and M. W. Naing, in *Proceedings of the 1st International Conference on Progress in Additive Manufacturing*, ed. C. K. Chua, W. Y. Yeong, M. J. Tan and E. Liu, 2014.
13 S. Jana and A. Lerman, *Biotechnol. Adv.*, 2015, **33**, 1503–1521.
14 J. M. Lee, S. L. Sing, E. Y. S. Tan and W. Y. Yeong, *Int. J. Bioprinting*, 2016, **2**, 27–36.
15 S. Bose, S. Vahabzadeh and A. Bandyopadhyay, *Mater. Today*, 2013, **16**, 496–504.
16 X. Wang, Y. Yan, Y. Pan, Z. Xiong, H. Liu, J. Cheng, F. Liu, F. Lin, R. Wu and R. Zhang, *Tissue Eng.*, 2006, **12**, 83–90.
17 Y. J. Tan, X. Tan, W. Y. Yeong and S. B. Tor, *Materials*, 2016, **9**, 893.
18 X. Cui, K. Breitenkamp, M. Finn, M. Lotz and D. D. D'Lima, *Tissue Eng., Part A*, 2012, **18**, 1304–1312.
19 H. Gudupati, M. Dey and I. Ozbolat, *Biomaterials*, 2016, **102**, 20–42.
20 R. E. Saunders and B. Derby, *Int. Mater. Rev.*, 2014, **59**, 430–448.
21 L. Koch, M. Gruene, C. Unger and B. Chichkov, *Curr. Pharm. Biotechnol.*, 2013, **14**, 91–97.
22 I. T. Ozbolat and M. Hospodiuk, *Biomaterials*, 2016, **76**, 321–343.
23 R. Suntornnond, E. Y. S. Tan, J. An and C. K. Chua, *Materials*, 2016, **9**, 756.
24 T. Xu, W. Zhao, J.-M. Zhu, M. Z. Albanna, J. J. Yoo and A. Atala, *Biomaterials*, 2013, **34**, 130–139.
25 I. T. Ozbolat and Y. Yu, *IEEE Trans. Biomed. Eng.*, 2013, **60**, 691–699.
26 D. G. Anderson, S. Levenberg and R. Langer, *Nat. Biotechnol.*, 2004, **22**, 863–866.
27 C. J. Flaim, S. Chien and S. N. Bhatia, *Nat. Methods*, 2005, **2**, 119–125.
28 C. Li, A. Faulkner-Jones, A. R. Dun, J. Jin, P. Chen, Y. Z. Xing, Z. Q. Yang, Z. B. Li, W. M. Shu, D. S. Liu and R. R. Duncan, *Angew. Chem., Int. Ed.*, 2015, **54**, 3957–3961.
29 Y. B. Lee, S. Polio, W. Lee, G. Dai, L. Menon, R. S. Carroll and S. S. Yoo, *Exp. Neurol.*, 2010, **223**, 645–652.
30 S. Moon, Y. G. Kim, L. Dong, M. Lombardi, E. Haeggstrom, R. V. Jensen, L. L. Hsiao and U. Demirci, *PLoS One*, 2011, **6**, e17455.
31 A. Faulkner-Jones, S. Greenhough, J. A. King, J. Gardner, A. Courtney and W. Shu, *Biofabrication*, 2013, **5**, 015013.
32 W. Lee, J. Pinckney, V. Lee, J. H. Lee, K. Fischer, S. Polio, J. K. Park and S. S. Yoo, *NeuroReport*, 2009, **20**, 798–803.
33 L. Horváth, Y. Umehara, C. Jud, F. Blank, A. Petri-Fink and B. Rothen-Rutishauser, *Sci. Rep.*, 2015, **5**, 7974.
34 V. Lee, G. Singh, J. P. Trasatti, C. Bjornsson, X. Xu, T. N. Tran, S.-S. Yoo, G. Dai and P. Karande, *Tissue Eng., Part C*, 2013, **20**, 473–484.
35 W. Lee, V. Lee, S. Polio, P. Keegan, J. H. Lee, K. Fischer, J. K. Park and S. S. Yoo, *Biotechnol. Bioeng.*, 2010, **105**, 1178–1186.
36 K. W. Binder, W. X. Zhao, T. Aboushwareb, D. Dice, A. Atala and J. J. Yoo, *J. Am. Coll. Surg.*, 2010, **211**, S76–S76.
37 C. J. Ferris, K. G. Gilmore and G. G. Wallace, *Appl. Microbiol. Biotechnol.*, 2013, **97**, 4243–4258.
38 J. M. Lee and W. Y. Yeong, *Virtual Phys. Prototyping*, 2015, **10**, 3–8.
39 E. Y. S. Tan and W. Y. Yeong, *Int. J. Bioprinting*, 2015, **1**, 49–56.
40 W. L. Ng, W. Y. Yeong and M. W. Naing, *Int. J. Bioprinting*, 2016, **2**, 53–62.
41 W. Lee, J. C. Debasitis, V. K. Lee, J.-H. Lee, K. Fischer, K. Edminster, J.-K. Park and S.-S. Yoo, *Biomaterials*, 2009, **30**, 1587–1595.
42 B. Derby, *Annu. Rev. Mater. Res.*, 2010, **40**, 395–414.
43 J. Sun, J. H. Ng, Y. H. Fuh, Y. San Wong, H. T. Loh and Q. Xu, *Microsyst. Technol.*, 2009, **15**, 1437–1448.

44 B. Derby and N. Reis, *MRS Bull.*, 2003, **28**, 815–818.
45 D. Chahal, A. Ahmadi and K. C. Cheung, *Biotechnol. Bioeng.*, 2012, **109**, 2932–2940.
46 I. Puhlev, N. Guo, D. R. Brown and F. Levine, *Cryobiology*, 2001, **42**, 207–217.
47 L. Koch, S. Kuhn, H. Sorg, M. Gruene, S. Schlie, R. Gaebel, B. Polchow, K. Reimers, S. Stoelting and N. Ma, *Tissue Eng., Part C*, 2009, **16**, 847–854.
48 B. Guillotin, A. Souquet, S. Catros, M. Duocastella, B. Pippenger, S. Bellance, R. Bareille, M. Rémy, L. Bordenave and J. Amédée, *Biomaterials*, 2010, **31**, 7250–7256.
49 B. Guillotin and F. Guillemot, *Trends Biotechnol.*, 2011, **29**, 183–190.
50 N. R. Schiele, D. T. Corr, Y. Huang, N. A. Raof, Y. Xie and D. B. Chrisey, *Biofabrication*, 2010, **2**, 032001.
51 F. Guillemot, B. Guillotin, A. Fontaine, M. Ali, S. Catros, V. Kériquel, J.-C. Fricain, M. Rémy, R. Bareille and J. Amédée-Vilamitjana, *MRS Bull.*, 2011, **36**, 1015–1019.
52 N. T. Kattamis, P. E. Purnick, R. Weiss and C. B. Arnold, *Appl. Phys. Lett.*, 2007, **91**, 171120.
53 D. O. Visscher, E. Farré-Guasch, M. N. Helder, S. Gibbs, T. Forouzanfar, P. P. van Zuijlen and J. Wolff, *Trends Biotechnol.*, 2016, **34**(9), 700–710.
54 D. Jang, D. Kim and J. Moon, *Langmuir*, 2009, **25**, 2629–2635.
55 L. Koch, A. Deiwick, S. Schlie, S. Michael, M. Gruene, V. Coger, D. Zychlinski, A. Schambach, K. Reimers and P. M. Vogt, *Biotechnol. Bioeng.*, 2012, **109**, 1855–1863.
56 A. Blaeser, D. F. Duarte Campos, U. Puster, W. Richtering, M. M. Stevens and H. Fischer, *Adv. Healthcare Mater.*, 2016, **5**, 326–333.
57 V. Mironov, V. Kasyanov and R. R. Markwald, *Curr. Opin. Biotechnol.*, 2011, **22**, 667–673.
58 K. Dubbin, Y. Hori, K. K. Lewis and S. C. Heilshorn, *Adv. Healthcare Mater.*, 2016, **5**(19), 2488–2492.
59 Y. Nishiyama, M. Nakamura, C. Henmi, K. Yamaguchi, S. Mochizuki, H. Nakagawa and K. Takiura, *J. Biomech. Eng.*, 2009, **131**, 035001.
60 C. Xu, W. Chai, Y. Huang and R. R. Markwald, *Biotechnol. Bioeng.*, 2012, **109**, 3152–3160.
61 M. Nakamura, A. Kobayashi, F. Takagi, A. Watanabe, Y. Hiruma, K. Ohuchi, Y. Iwasaki, M. Horie, I. Morita and S. Takatani, *Tissue Eng.*, 2005, **11**, 1658–1666.
62 T. Jungst, W. Smolan, K. Schacht, T. Scheibel and J. r. Groll, *Chem. Rev.*, 2015, **116**, 1496–1539.
63 J. E. Fromm, *IBM J. Res. Dev.*, 1984, **28**, 322–333.
64 J. Malda, J. Visser, F. P. Melchels, T. Jüngst, W. E. Hennink, W. J. Dhert, J. Groll and D. W. Hutmacher, *Adv. Mater.*, 2013, **25**(36), 5011–5028.
65 T. Mao, D. Kuhn and H. Tran, *AIChE J.*, 1997, **43**, 2169–2179.
66 H. Mizuno, M. Tobita and A. C. Uysal, *Stem Cells*, 2012, **30**, 804–810.
67 R. O. Oreffo, C. Cooper, C. Mason and M. Clements, *Stem Cell Rev.*, 2005, **1**, 169–178.
68 K. I. Pappa and N. P. Anagnou, *Regenerative medicine*, 2009, **4**(3), 423–433.
69 C. Xu, M. Zhang, Y. Huang, A. Ogale, J. Fu and R. R. Markwald, *Langmuir*, 2014, **30**, 9130–9138.
70 F. Xu, J. Wu, S. Wang, N. G. Durmus, U. A. Gurkan and U. Demirci, *Biofabrication*, 2011, **3**, 034101.
71 T. Hart, A. Zhao, A. Garg, S. Bolusani and E. M. Marcotte, *PLoS One*, 2009, 4.
72 T. G. Fernandes, S. J. Kwon, M. Y. Lee, D. S. Clark, J. M. S. Cabral and J. S. Dordick, *Anal. Chem.*, 2008, **80**, 6633–6639.
73 T. G. Fernandes, S. J. Kwon, S. S. Bale, M. Y. Lee, M. M. Diogo, D. S. Clark, J. M. S. Cabral and J. S. Dordick, *Biotechnol. Bioeng.*, 2010, **106**, 106–118.
74 M. Y. Lee, R. A. Kumar, S. M. Sukumaran, M. G. Hogg, D. S. Clark and J. S. Dordick, *Proc. Natl. Acad. Sci. U. S. A.*, 2008, **105**, 59–63.
75 P. Bianco and P. G. Robey, *Nature*, 2001, **414**, 118–121.
76 J. M. Lee, M. Zhang and W. Y. Yeong, *Microfluid. Nanofluid.*, 2016, **20**, 1–15.
77 C. Streuli, *Curr. Opin. Cell Biol.*, 1999, **11**, 634–640.
78 G.-S. Huang, P.-S. Hsieh, C.-S. Tseng and S.-h. Hsu, *Biomater. Sci.*, 2014, **2**, 1652–1660.
79 J. J. Rice, M. M. Martino, L. De Laporte, F. Tortelli, P. S. Briquez and J. A. Hubbell, *Adv. Healthcare Mater.*, 2013, **2**, 57–71.
80 M. M. Martino, P. S. Briquez, E. Güç, F. Tortelli, W. W. Kilarski, S. Metzger, J. J. Rice, G. A. Kuhn, R. Müller and M. A. Swartz, *Science*, 2014, **343**, 885–888.
81 C. W. Pouton and J. M. Haynes, *Nat. Rev. Drug Discovery*, 2007, **6**, 605–616.
82 C. E. Murry and G. Keller, *Cell*, 2008, **132**, 661–680.
83 C. Cerdan, S. H. Hong and M. Bhatia, *Curr. Protoc. Stem Cell Biol.*, 2007, 1D. 2.1–1D. 2.16.
84 A. P. Napolitano, D. M. Dean, A. J. Man, J. Youssef, D. N. Ho, A. P. Rago, M. P. Lech and J. R. Morgan, *Biotechniques*, 2007, **43**, 494.
85 Y. T. Matsunaga, Y. Morimoto and S. Takeuchi, *Adv. Mater.*, 2011, 23.
86 R. Peerani, B. M. Rao, C. Bauwens, T. Yin, G. A. Wood, A. Nagy, E. Kumacheva and P. W. Zandstra, *EMBO J.*, 2007, **26**, 4744–4755.
87 J. Park, C. H. Cho, N. Parashurama, Y. Li, F. Berthiaume, M. Toner, A. W. Tilles and M. L. Yarmush, *Lab Chip*, 2007, **7**, 1018–1028.
88 D. J. Tobin, *Chem. Soc. Rev.*, 2006, **35**, 52–67.
89 W. L. Ng, W. Y. Yeong and M. W. Naing, *J. Tissue Sci. Eng.*, 2015, **6**, 1–9.
90 S. Moon, S. K. Hasan, Y. S. Song, F. Xu, H. O. Keles, F. Manzur, S. Mikkilineni, J. W. Hong, J. Nagatomi, E. Haeggstrom, A. Khademhosseini and U. Demirci, *Tissue Eng., Part C*, 2010, **16**, 157–166.
91 F. Xu, S. J. Moon, A. E. Emre, E. S. Turali, Y. S. Song, S. A. Hacking, J. Nagatomi and U. Demirci, *Biofabrication*, 2010, **2**, 014105.
92 A. C. Wan, *Trends Biotechnol.*, 2016, **34**(9), 711–721.

93 I. Martin, D. Wendt and M. Heberer, *Trends Biotechnol.*, 2004, **22**, 80–86.
94 Y. Zhang, Y. Yu, A. Akkouch, A. Dababneh, F. Dolati and I. T. Ozbolat, *Biomater. Sci.*, 2015, **3**, 134–143.
95 Z. Min, Z. Shichang, X. Chen, Z. Yufang and Z. Changqing, *Biomater. Sci.*, 2015, **3**, 1236–1244.
96 M. Wang, J. He, Y. Liu, M. Li, D. Li and Z. Jin, *Int. J. Bioprinting*, 2015, **1**, 15–26.
97 S. Monstrey, H. Hoeksema, J. Verbelen, A. Pirayesh and P. Blondeel, *Burns*, 2008, **34**, 761–769.
98 A. Skardal, D. Mack, E. Kapetanovic, A. Atala, J. D. Jackson, J. Yoo and S. Soker, *Stem Cells Transl. Med.*, 2012, **1**, 792–802.
99 M. E. Pepper, V. Seshadri, T. C. Burg, K. J. Burg and R. E. Groff, *Biofabrication*, 2012, **4**, 011001.
100 M. het Panhuis, *Biomater. Sci.*, 2013, **1**, 224–230.
101 Z. Wang and J. M. Belovich, *Biotechnol. Prog.*, 2010, **26**, 1361–1366.
102 H. Lin, D. Zhang, P. G. Alexander, G. Yang, J. Tan, A. W.-M. Cheng and R. S. Tuan, *Biomaterials*, 2013, **34**, 331–339.
103 J. Jia, D. J. Richards, S. Pollard, Y. Tan, J. Rodriguez, R. P. Visconti, T. C. Trusk, M. J. Yost, H. Yao and R. R. Markwald, *Acta Biomater.*, 2014, **10**, 4323–4331.
104 A. Blaeser, D. F. Duarte Campos, U. Puster, W. Richtering, M. M. Stevens and H. Fischer, *Adv. Healthcare Mater.*, 2015, **5**(3), 326–333.
105 A. Tirella and A. Ahluwalia, *Biotechnol. Prog.*, 2012, **28**, 1315–1320.
106 D. Quéré, *Nature*, 2005, **435**, 1168–1169.
107 L. Xu, W. W. Zhang and S. R. Nagel, *Phys. Rev. Lett.*, 2005, **94**, 184505.
108 J. Malda, J. Visser, F. P. Melchels, T. Jüngst, W. E. Hennink, W. J. Dhert, J. Groll and D. W. Hutmacher, *Adv. Mater.*, 2013, **25**, 5011–5028.
109 T. Billiet, M. Vandenhaute, J. Schelfhout, S. Van Vlierberghe and P. Dubruel, *Biomaterials*, 2012, **33**, 6020–6041.
110 A. Skardal and A. Atala, *Ann. Biomed. Eng.*, 2015, **43**, 730–746.
111 S. Wang, J. M. Lee and W. Y. Yeong, *Int. J. Bioprinting*, 2015, **1**, 3–14.
112 Z. X. Khoo, J. E. M. Teoh, Y. Liu, C. K. Chua, S. Yang, J. An, K. F. Leong and W. Y. Yeong, *Virtual Phys. Prototyping*, 2015, **10**, 103–122.
113 C. Frantz, K. M. Stewart and V. M. Weaver, *J. Cell Sci.*, 2010, **123**, 4195–4200.
114 B. E. Uygun, A. Soto-Gutierrez, H. Yagi, M.-L. Izamis, M. A. Guzzardi, C. Shulman, J. Milwid, N. Kobayashi, A. Tilles and F. Berthiaume, *Nat. Med.*, 2010, **16**, 814–820.
115 L. Flynn, *Biomaterials*, 2010, **31**, 4715–4724.
116 F. Pati, J. Jang, D.-H. Ha, S. W. Kim, J.-W. Rhie, J.-H. Shim, D.-H. Kim and D.-W. Cho, *Nat. Commun.*, 2014, 5.
117 S. F. Badylak, D. J. Weiss, A. Caplan and P. Macchiarini, *Lancet*, 2012, **379**, 943–952.
118 T. Xu, K. W. Binder, M. Z. Albanna, D. Dice, W. Zhao, J. J. Yoo and A. Atala, *Biofabrication*, 2012, **5**, 015001.
119 G. Kim, J. Son, S. Park and W. Kim, *Macromol. Rapid Commun.*, 2008, **29**(19), 1577–1581.
120 C. J. Bettinger, R. Langer and J. T. Borenstein, *Angew. Chem., Int. Ed.*, 2009, **48**, 5406–5415.
121 C. C. Berry, G. Campbell, A. Spadiccino, M. Robertson and A. S. Curtis, *Biomaterials*, 2004, **25**, 5781–5788.
122 E. K. Yim, S. W. Pang and K. W. Leong, *Exp. Cell Res.*, 2007, **313**, 1820–1829.